Filling Knowledge Gaps for Mimivirus Entry, Uncoating, and Morphogenesis

Ana Claudia Dos Santos Pereira Andrade, Rodrigo Araujo Lima Rodrigues, Graziele Pereira Oliveira, Ketyllen Reis Andrade, Claudio Antonio Bonjardim, Bernard La Scola, Erna Geessien Kroon, Jonatas Santos Abrahao

AMERICAN SOCIETY FOR MICROBIOLOGY | Journal of Virology®

VIRUS-CELL INTERACTIONS

Filling Knowledge Gaps for Mimivirus Entry, Uncoating, and Morphogenesis

Ana Cláudia dos Santos Pereira Andrade,[a] Rodrigo Araújo Lima Rodrigues,[a] Graziele Pereira Oliveira,[a] Kétyllen Reis Andrade,[b] Cláudio Antônio Bonjardim,[a] Bernard La Scola,[c] Erna Geessien Kroon,[a] Jônatas Santos Abrahão[a]

Departamento de Microbiologia, Instituto de Ciências Biológicas, Universidade Federal de Minas Gerais, Belo Horizonte, Minas Gerais, Brazil[a]; Laboratório de Imunopatologia de Doenças Virais, Centro de Pesquisas René Rachou—Fiocruz, Minas Gerais, Brazil[b]; URMITE, CNRS UMR 6236, IRD 3R198, Aix Marseille Universite, Marseille, France[c]

ABSTRACT Since the discovery of mimivirus, its unusual structural and genomic features have raised great interest in the study of its biology; however, many aspects concerning its replication cycle remain uncertain. In this study, extensive analyses of electron microscope images, as well as biological assay results, shed light on unclear points concerning the mimivirus replication cycle. We found that treatment with cytochalasin, a phagocytosis inhibitor, negatively impacted the incorporation of mimivirus particles by *Acanthamoeba castellanii*, causing a negative effect on viral growth in amoeba monolayers. Treatment of amoebas with bafilomicin significantly impacted mimivirus uncoating and replication. In conjunction with microscopic analyses, these data suggest that mimiviruses indeed depend on phagocytosis for entry into amoebas, and particle uncoating (and stargate opening) appears to be dependent on phagosome acidification. In-depth analyses of particle morphogenesis suggest that the mimivirus capsids are assembled from growing lamellar structures. Despite proposals from previous studies that genome acquisition occurs before the acquisition of fibrils, our results clearly demonstrate that the genome and fibrils can be acquired simultaneously. Our data suggest the existence of a specific area surrounding the core of the viral factory where particles acquire the surface fibrils. Furthermore, we reinforce the concept that defective particles can be formed even in the absence of virophages. Our work provides new information about unexplored steps in the life cycle of mimivirus.

IMPORTANCE Investigating the viral life cycle is essential to a better understanding of virus biology. The combination of biological assays and microscopic images allows a clear view of the biological features of viruses. Since the discovery of mimivirus, many studies have been conducted to characterize its replication cycle, but many knowledge gaps remain to be filled. In this study, we conducted a new examination of the replication cycle of mimivirus and provide new evidence concerning some stages of the cycle which were previously unclear, mainly entry, uncoating, and morphogenesis. Furthermore, we demonstrate that atypical virion morphologies can occur even in the absence of virophages. Our results, along with previous data, allow us to present an ultimate model for the mimivirus replication cycle.

KEYWORDS mimivirus, electron microscopy, replication cycle, phagocytosis, fibril acquisition area

The giant Acanthamoeba polyphaga mimivirus (APMV), which is associated with amoebas of the *Acanthamoeba* genus, was isolated in 2003 and astonished the scientific community with unusual structural and genomic features within the virosphere (1, 2). In subsequent years, several mimivirus-like viruses were uncovered in different parts of the world, thus expanding the *Mimiviridae* family, especially the

Received 2 August 2017 **Accepted** 23 August 2017

Accepted manuscript posted online 6 September 2017

Citation Andrade ACDSP, Rodrigues RAL, Oliveira GP, Andrade KR, Bonjardim CA, La Scola B, Kroon EG, Abrahão JS. 2017. Filling knowledge gaps for mimivirus entry, uncoating, and morphogenesis. J Virol 91:e01335-17. https://doi.org/10.1128/JVI.01335-17.

Editor Rozanne M. Sandri-Goldin, University of California, Irvine

Address correspondence to Jônatas Santos Abrahão, jonatas.abrahao@gmail.com.

A.C.D.S.P.A., R.A.L.R., and G.P.O. contributed equally to this work.

Mimivirus genus (3–7). These viruses have some genetic differences which define three distinct lineages (A, B, and C), but they are structurally similar.

Mimiviruses are composed of a particle with a pseudoicosahedral symmetry, 750-nm diameter, and a genome of double-stranded DNA of approximately 1.2 Mb (2, 8). They have a capsid of 500 nm that is formed of multiple protein layers and a lipid membrane surrounding an inner proteinaceous core, which contains the genome. A star-shaped projection is present on the capsid, from which the viral genome is released into the host cytoplasm; this is referred to as the stargate and represents a unique feature of mimiviruses (9). In addition, a dense layer of 125-nm-long glycoproteic fibers covers the viral surface and is important for viral attachment to different organisms, including amoeboid hosts (10).

Given the large size of mimiviruses, it has been proposed and largely accepted that the replication cycle of these viruses begins with phagocytosis of viral particles by *Acanthamoeba* spp. cells (11, 12). Information is lacking concerning the set of events that occurs between virion entry and stargate opening, but there is evidence that after opening of the stargate, the virion inner lipid membrane merges with that of the entry vesicle and releases the viral seed into the amoeba's cytoplasm. A typical viral eclipse phase is then established, during which viral particles are not visible in the cell (11, 13). The viral seed releases the DNA, promoting a reorganization of the host cytoplasm with further formation of viral factories (VF), where the virus genome is replicated and transcribed and new particles are assembled (13, 14). Based on atomic force microscopy, Kuznetsov and colleagues proposed a model for morphogenesis of mimivirus particles (15). In the model, capsid assembly occurs on the VF surface in a temporal fashion; assembly is initiated by the formation of the stargate portal, followed by thickening of the protein layer in its immediate vicinity. Before capsid formation is complete, the capsids are filled with DNA and other macromolecules through a stargate distal portal. Once the genome is enclosed within the capsid, an integument protein layer attaches to the capsid, on which a coating of fibrils then adheres to the entire viral surface (15). The involvement of the nucleus during the replication of these viruses is still unclear. Suzan-Monti and colleagues (11) suggested that APMV replication is nucleocytoplasmic, although other studies have argued that replication occurs exclusively in the host cell cytoplasm (13).

Mimiviruses have been studied for several years; nevertheless, some aspects regarding their biology remain unclear. Based on biological assays in conjunction with extensive electron microscopic analyses, now we are able to shed new light on the mimivirus replication cycle.

RESULTS

Biological assays suggest mimivirus entry into amoebas by phagocytosis. Although mimiviruses have been studied for more than a decade, some aspects of their replication cycle remain uncertain, such as their entry into natural hosts. Due to its large size (~700 nm), it has been proposed and widely accepted that mimivirus enters *Acanthamoeba* cells by phagocytosis (11, 13). However, to our knowledge there has been no biological demonstration of this process. Here, we confirm this hypothesis by using experimental data. Pretreatment of cells with cytochalasin D significantly decreased the titers and numbers of particles incorporated into cells infected with APMV (Fig. 1A and B). *Marseillevirus marseillevirus* (MsV) titers and particle incorporation were not reduced after this treatment, since isolated purified particles exploit the endocytic pathway (16). Pretreatment with bafilomycin also resulted in a significant reduction in APMV and MsV titers (Fig. 1C). Bafilomycin is a specific inhibitor of vacuolar-type H^+/ATPase that prevents phagosome and endosome acidification (17). Therefore, these results demonstrated that APMV replication is dependent on the acidification of phagosomes for the uncoating step. The acidification of the entry compartment is also important for MsV (16). These results have been corroborated by several transmission electron microscope (TEM) images that show the occurrence of phagosome-lysosome fusion, subsequent stargate opening, and release of the viral seed (Fig. 1D to L). Taken

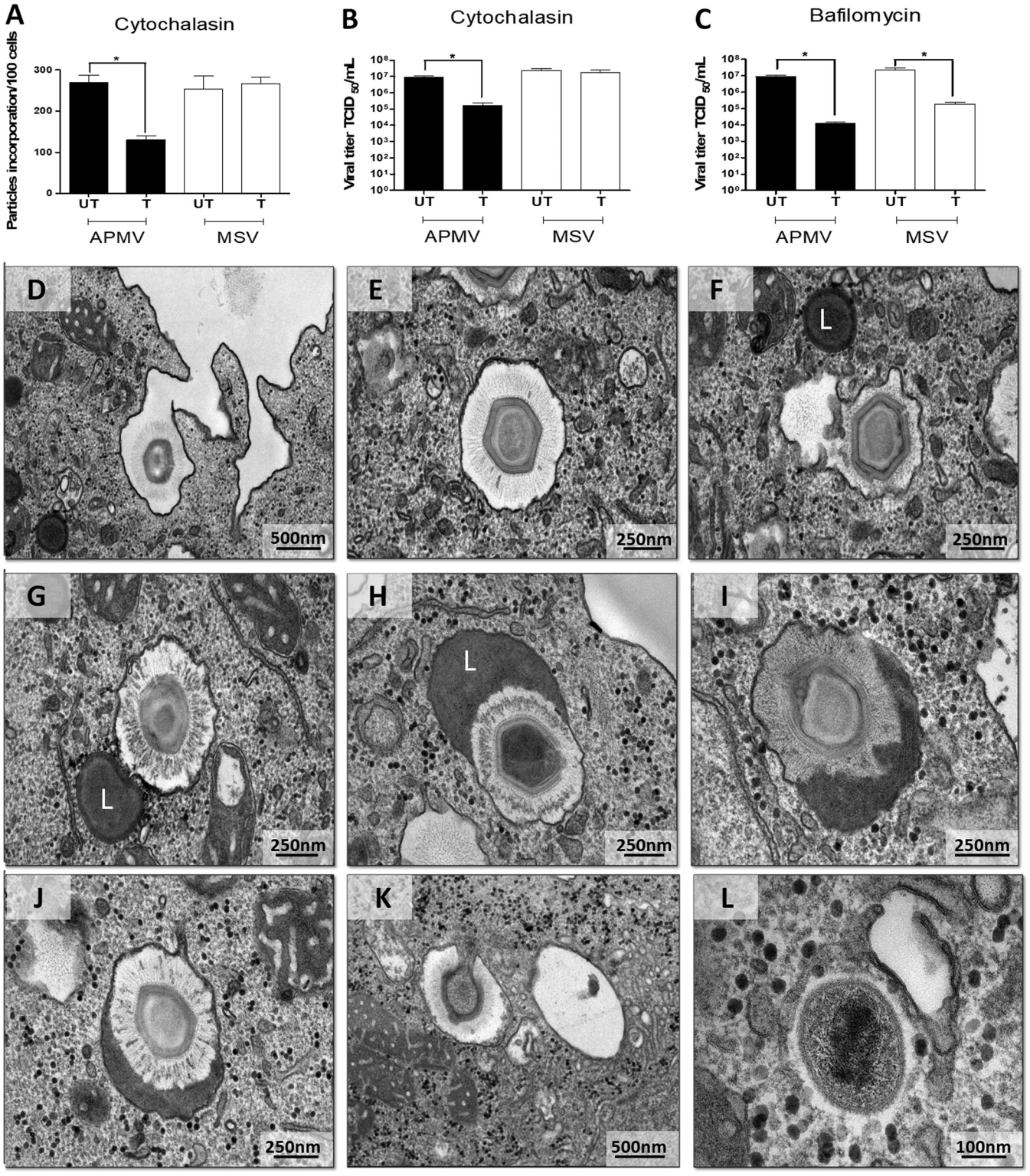

FIG 1 Mimivirus entry into the host cell by phagocytosis and uncoating depends on acidification of the phagosome. (A to C) The impact of cytochalasin D and bafilomycin on mimivirus replication. Treatment with cytochalasin D and bafilomycin decreased the mimivirus titers and particle incorporation. MsV was used as a control, and its titer was not reduced after the treatment with cytochalasin D but was reduced with treatment with bafilomycin. (D to L) Transmission electron microscopy images of mimivirus particles entering cells by phagocytosis (D to F), the phagosome-lysosome fusion (F to J), stargate opening (K), and release of the viral seed (L). The inhibitory assays were performed in triplicate. Error bars indicate standard deviations. *, $P < 0.05$ (two-tailed Student's *t* test). UN, untreated cells; T, treated cells; L, lysosome.

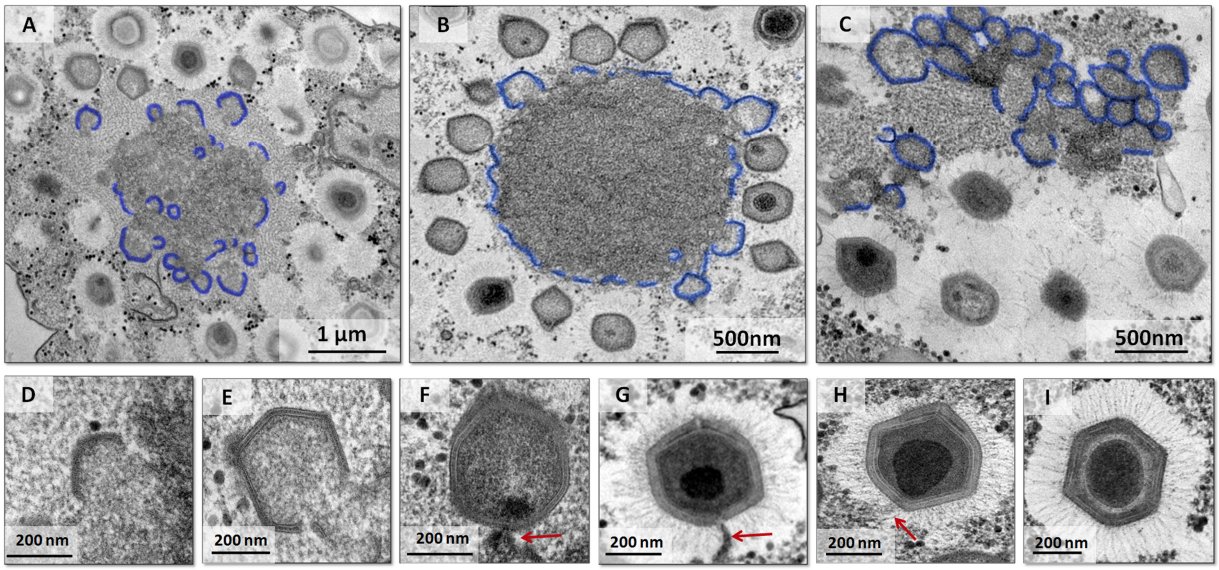

FIG 2 Growing lamellar structures seem to be important to mimivirus capsid assembly. (A to C) Growing lamellar structures with different sizes in the viral factory, demonstrating the viral crescent-like structures (in blue). The smaller blocks are observed in the interiors of the viral factories, and more complete particles are shown in the periphery of the factory. (D to I) Transmission electron microscopy images showing stages of mimivirus particle formation, as the particle grows in thickness and complexity. Images show the viral crescent (D), particles without a genome (E), fibrils (E and F), particles acquiring genome (red arrows) and fibrils (F to H), and finally complete mimivirus particle formation (I).

together, these results support the view that APMV entry into *Acanthamoeba* cells may occur via phagocytosis.

Capsids are assembled from growing lamellar structures. After mimivirus enters amoeba cells and delivers the viral seed, early DNA replication and transcription appear to take place exclusively in the host cytoplasm, moments before the formation of a mature VF (13). Once a mature VF is formed, the morphogenesis step is initiated. It has been proposed that the formation of the mimivirus capsid begins with the formation of the stargate, followed by thickening of the protein layer in its immediate vicinity (15). However, it is not yet clear how expansion of this protein layer occurs. Through analyses of TEM images of VF at different time points postinfection, we observed the presence of several lamellar structures preceding capsid formation, with different sizes in the inner part of the VF (Fig. 2A to C and 3A and B). Mutsafi and colleagues in 2013 showed the formation of multivesicular bodies and membrane sheets from the endoplasmic reticulum (ER) in the outermost zone of the mimivirus VF, the membrane assembly zone (18). Our TEM images provide evidence for the formation of lamellar structures, not only on the periphery of the VF but also in its interior (Fig. 2A to C and 3A and B), which is in accordance with the data of Mutsafi and colleagues. It is noteworthy that after assembly of the complete particle in the later stages of infection (~7 h postinfection), the crescents were no longer observed. These lamellar structures, which began in a way analogous to the crescents described for poxviruses and marseilleviruses, increased in complexity until reaching the VF periphery and moving to the next stages of virion morphogenesis (Fig. 2D to I): incorporation of DNA and surface fibrils. In contrast to lamellar capsid-forming structures, the main component of viral factories is a globular aspect, likely formed by DNA, membranes, and enzymes (Fig. 3A and B).

Dynamic acquisition of surface fibrils: the fibril acquisition area (FAA). The mature mimivirus particle is covered by fibrils of lengths ranging from 125 nm to 140 nm (8). A previous study based on atomic force microscopy proposed that the surface fibers are acquired by viral capsids when they pass sequentially through a membrane embedded with integument protein and then through a membrane containing surface fibers (15). In this model, layers of integument and fibrils are acquired

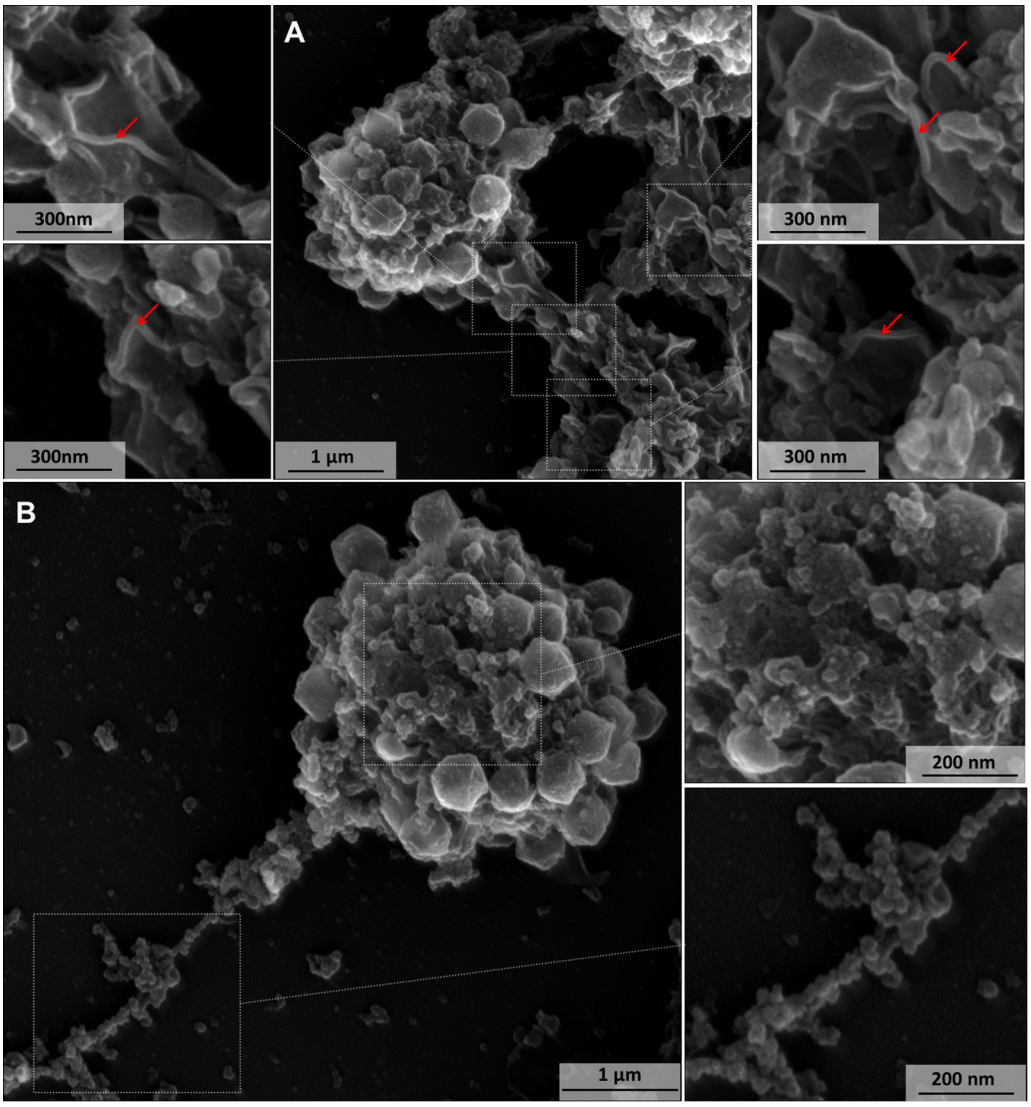

FIG 3 Scanning microscopy of a disrupted mimivirus viral factory. (A) Lamellar structures related to capsid morphogenesis. The red arrows indicate the lamelar structures around the viral factory. (B) In contrast to lamellar capsid-forming structures, the main component of VF presents a globular aspect, likely formed by DNA, membranes, and enzymes.

as an envelope involving the capsid. The same study also suggested that the integument protein layer is acquired near the VF but the fibril layer is acquired near the cellular periphery, and the source of these fibrils has not been demonstrated (15).

We noticed a very clear phenomenon regarding the dynamics of fibril acquisition, leading us to an overview of this step. In TEM images, it is possible to observe at the periphery of the VF a less-electron-dense region of an apparent fibrillar nature, which we named the fibril acquisition area (Fig. 4A and B). This arrangement is very clear and can be verified in almost all VF. During particle morphogenesis, newly formed capsids pass through this region where the particles acquire the fibrils. This was evident when we observed particles at the edge of the FAA, which had fibrils only in the upper portion, suggesting that this fibrillar region provides the fibrils for these particles (Fig. 5). In addition, the particles that had already passed through this region had fibrils all over their surface (Fig. 5). In the stages where we found few formed viral particles, the dimension of FAA was larger, and as long as the amount of newly formed particles increased, this region was reduced in size (Fig. 4A and B and 5). This phenomenon suggests that, as viral particles are formed, the fibrillar material that gives rise to fibrils

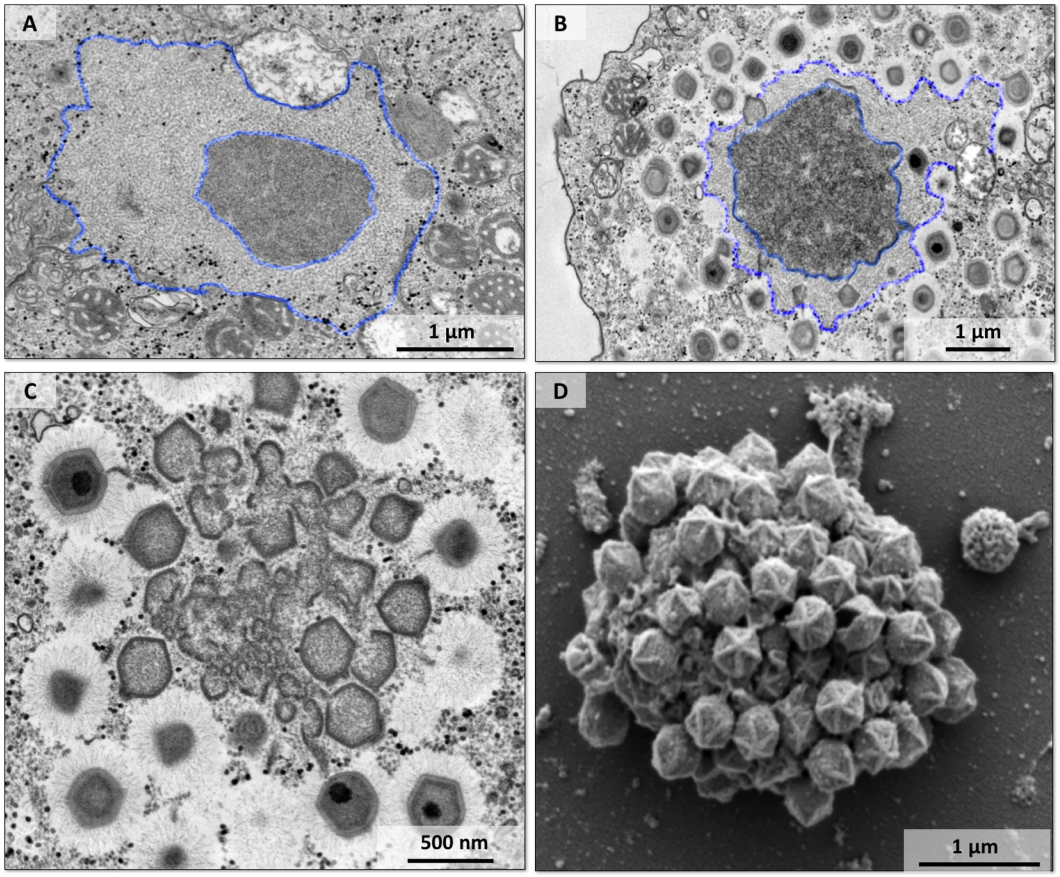

FIG 4 An area of fibril acquisition is present in the periphery of the viral factory. (A to C) Transmission electron microscopy images of the viral factory of mimivirus with a less-electron-dense area surrounding the periphery of the factory that decreased in size during particle morphogenesis. A fibril acquisition area is shown at early (A) and mature (B) stages of viral factory formation (highlighted by blue lines). (C) Mimivirus particles with fibrils in the periphery of the viral factory and particles without fibrils inside the factory before passing through the fibril acquisition area. (D) Scanning electron microscopy image of a viral factory with particles without fibrils (before fibril acquisition) and a prominent stargate.

is consumed. The TEM images of the VF showed the viral capsids forming blocks, growing in thickness and complexity as they migrated to the outermost part of the VF and acquiring fibrils when they passed through the FAA (Fig. 2 and 4C). In a scanning electron microscope (SEM) image, it was not possible to view the FAA, and the particles were being assembled before fibril acquisition (Fig. 4D). Notably, all particles were without fibrils and displayed a prominent stargate (Fig. 4D).

Together, the data presented here lead us to suggest that the fibrils are acquired in the FAA, not near the cellular periphery as previously suggested (15). This view was also supported by the presence of various viral particles with fibrils in the cell cytoplasm. In addition, we did not observe the acquisition of the fibril layer during passage through a membrane, as previously described (15). Our images suggest that fibrils are acquired by the capsid when they pass through a region presenting the preformed fibrils. The full composition of the FAA, as well as the mechanism(s) of fibril binding in the protein capsid, still require further investigation.

Simultaneous occurrence of genome incorporation and fibril acquisition. The processes of release and packaging of the viral genome in mimiviruses have been analyzed in previous studies (9, 13, 15). It has been demonstrated that genome delivery occurs through the stargate and packaging occurs through the opposite portal (9). This strategy is different from that of other icosahedral viruses, in which a single vertex-portal system plays a crucial role in both genome release and packaging (9, 19). The viral genome is acquired at the periphery of the VF during the morphogenesis step

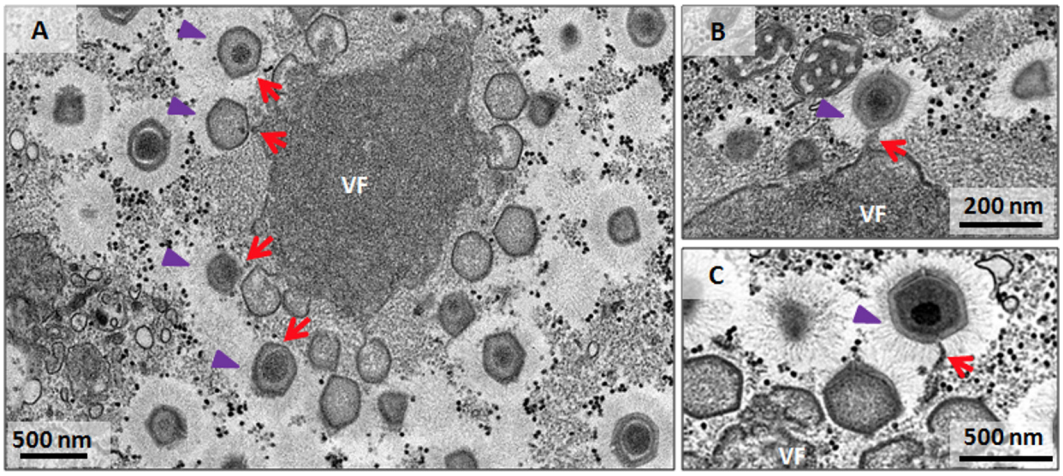

FIG 5 Fibril acquisition and genome incorporation can occur simultaneously. Transmission electron microscopy images of mature viral factories indicate genome incorporation (red arrows) simultaneous to the acquisition of fibrils (purple arrowheads). Viral particles are not fully covered by the fibrils (only half of each particle has fibrils), and the genome is still being packaged. The image shows that the viral genome is acquired at the periphery of the viral factory, at the FAA.

(11, 13). The particles that have already acquired a genome have a more-electron-dense region inside them, while those that have not yet acquired the genome do not exhibit this feature (Fig. 2E to H and 5). It was previously proposed that the formation of the capsid, acquisition of the genome, and acquisition of fibrils by mimivirus particles occur sequentially in this order (15). According to this model, the genome enters into the empty capsid, the nucleic acid condenses inside, and the entry portal is sealed, completing the assembly of the capsid. Subsequently, upper structural layers of integument and fibrils are acquired to form a mature particle (15).

Our data strongly suggest an alternative view of these events during mimivirus morphogenesis. In transverse sections of the VF, we clearly observed particles which were fully or partially covered by fibrils still acquiring the genome (Fig. 4C and 5). Further TEM images showed particles that had already passed through the fibrillar region and were therefore covered by fibrils and were acquiring the genome in the region opposite the stargate (Fig. 4C and 5). It is noteworthy that some viral particles were not fully covered by the fibrils (only half of the particle has fibrils), and the genome was still being packaged (Fig. 5). In contrast to what has been previously proposed, our data suggest that no sequential order of events occurs in the final steps of mimivirus morphogenesis concerning genome acquisition and fibril incorporation. It is possible that fibrils attach to some viral particles after full genome acquisition, but most of the images presented here lead us to support the hypothesis that the acquisition of the genome occurs concomitantly with the acquisition of the surface fibrils.

Viral particles with unusual morphologies. The particles of viral progeny were mostly well formed with a typical morphology. However, particles with unusual structures were also observed. TEM images showed unusual projections starting from the capsid or on its sides and from capsids without typical symmetry (Fig. 6A to C). In addition, an assembled empty capsid in the center of the VF was observed, an unexpected finding considering the particular stage of the virus replication cycle (Fig. 6D). Particles with an altered fibril arrangement were also identified, and SEM images showed particles with a nonuniform distribution of fibrils (Fig. 6E and F).

It has been shown that virophages affect the replication cycle of mimiviruses, decreasing amoeba lysis and generating particles with abnormal morphologies (20–22). Some particles showed capsid layers that asymetrically accumulated on the viral particle or harbored fibrils in only one part of the capsid. Sputnik was the first virophage described which infected a strain of mimivirus (20). Since then, other virophages have

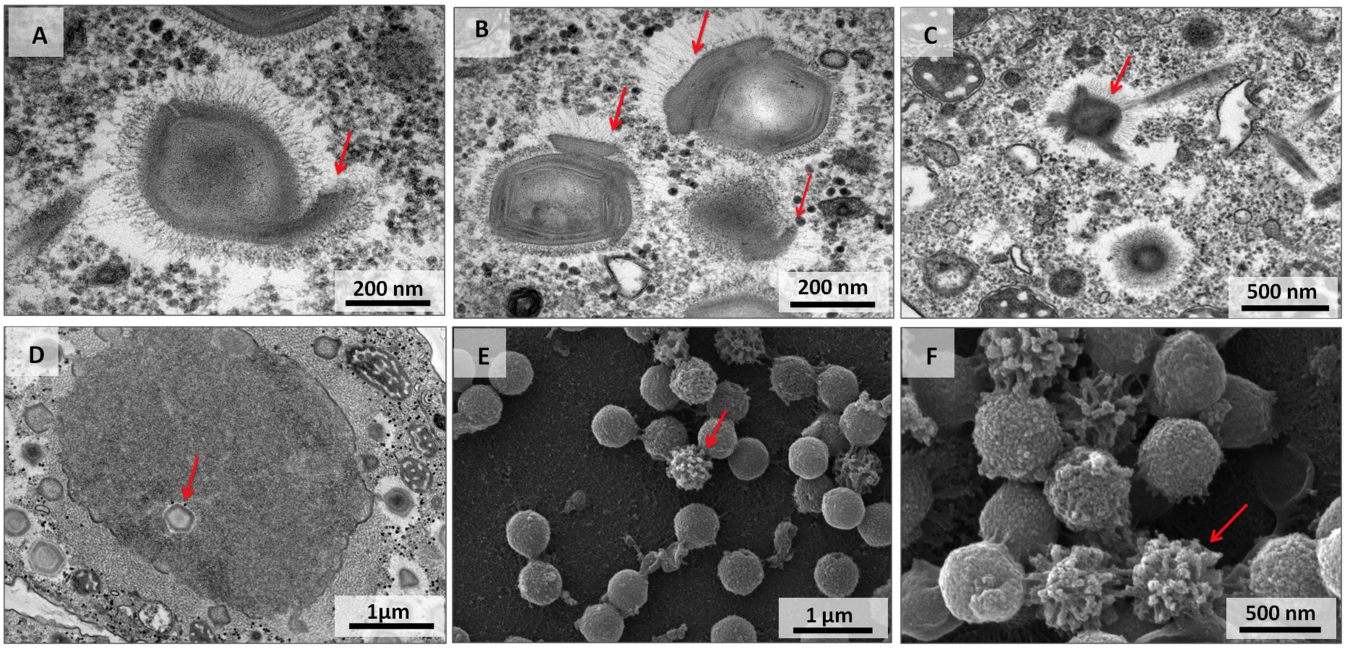

FIG 6 Defective particles in the mimivirus replication cycle in the absence of virophages. (A to D) Transmission electron microscopy images of mimivirus particles with atypical morphology (A to C) and an unusual localization of assembled empty capsid in the center of the viral factory (D). (E and F) Scanning electron microscopy images of particles with a nonuniform distribution of fibrils. Red arrows point to unusual features.

been described, thus reinforcing this new class of viruses (5, 22, 23). Virophages cannot replicate alone in amoebas, but they can replicate in the mimiviral VF. They have a small diameter (50 nm) and an icosahedral capsid, but they can be visualized in TEM images in VF and even within viral particles (20, 22). However, none of the images analyzed in this study exhibited signs of the presence of virophages, even in those images in which defective particles were found. To date, our APMV stocks have been tested by PCR for the presence of Sputniks and Zamilon, but we failed to amplify any virophage gene.

As previously demonstrated, different multiplicities of infection (MOI) used for mimivirus production resulted in distinct proportions of infectious particles in newly formed progeny, whereas the most efficacious way to produce infectious mimivirus particles is to use a low MOI (24). Although we followed this strategy during sample preparation for TEM analyses, multiple particles can infect the same cell and saturate the cellular machinery, thus generating defective particles. This is probably a usual phenomenon in nature, and the formation of defective particles, even in the absence of virophages, may be more frequent than previously thought (20, 24).

DISCUSSION

A better comprehension of the biology of a virus is achieved with basic investigations of its life cycle. Viruses are a highly heterogeneous group of organisms and present different replication strategies. In general, DNA viruses replicate in the host cell nucleus, while RNA viruses replicate within the cell cytoplasm. However, there are some exceptions, such as some members of the putative *Megavirales* order: poxviruses and iridoviruses, for instance (25). These double-stranded DNA viruses replicate in the host cytoplasm, wherein they establish a complex viral factory as an intracellular compartment in which both genome replication and viral morphogenesis occur (26). The giant mimiviruses share this same peculiarity. Studies have been conducting to better comprehend the replication cycle of these viruses, wherein models that explain this virus life cycle are constantly being updated (11, 13, 15, 18). In this study, we filled some gaps in the data concerning mimiviruses and introduced some data relating to entry, uncoating, and morphogenesis in the mimivirus replication cycle.

Mimiviruses have a diameter of approximately 700 nm and infect free-living amoe-

bas from the *Acanthamoeba* genus, which are protists that feed by phagocytosis (8, 27). The large size of mimiviruses associated with their host's life style, along with electron microscopy images, led to the assumption that these viruses enter host cells by phagocytosis, but until now there were no biological data to validate these assumptions. Inhibition of phagocytosis with cytochalasin D allowed us to observe a significant reduction in mimivirus entry, which was not observed with marseilleviruses (viruses of ~200-nm diameter) (Fig. 1A and B). With supported from TEM images, the data show that mimiviruses entered amoeba cells by phagocytosis, while marseilleviruses explored alternative pathways, as previously demonstrated (16). Furthermore, our data suggested the possible importance of phagosome acidification for mimivirus uncoating (Fig. 1C to L). In the presence of bafilomycin, viral replication was impaired. It is possible that a decrease in pH after formation of the phagolysosome is the triggering factor to the opening of the mimivirus stargate, thus allowing the release of viral seed into the host cytoplasm. Nevertheless, it remains uncertain which pH is ideal for triggering this process, or whether enzymes present in the lysosomes are essential for this process.

After release of the viral seed, the DNA replication and transcription take place in early VF (13). It is possible that nuclear factors are involved in this step, but further evidence is needed (28). Assembly of new viral particles takes place inside a mature VF. Previous studies have shown that membranes from the endoplasmic reticulum (ER) migrate toward the edge of the VF and act as scaffolding for the assembly of capsids, which would occur by acquisition of individual pentameric units in sequence (15). Our data corroborate this theory, demonstrating the existence and expansion of lamellar structures, in an way analogous to that of crescents described for poxviruses and marseilleviruses (Fig. 2 and 3) (16, 29). It is possible that membranes from the ER migrate into the VF, wherein they act as scaffolding for protein blocks. These structures increase in size by incorporation of proteins which move away from the core of the VF, until they pass through a fibrillar aspect area, which we named the fibril acquisition area, wherein the new viral particles acquire surface fibrils (Fig. 4 and 5). This hypothesis was strengthened when we systematically observed the reduction of the fibrillar area after release of viral particles from the VF, suggesting that a fibrillar matrix is continuously consumed as the particles pass through it. Curiously, fibril proteins were not detected in isolated VF analyzed via proteomic approaches (14). It is possible that a large fraction of that region was lost during the purification process of the factories, thus hampering the detection of fibrils by this method. Our hypothesis for the acquisition of fibrils by mimiviruses relies on a different or maybe complementary way to that proposed by Kuznetsov and colleagues, who proposed that a layer containing the fibrils involves the viral capsid in a region distant from the VF (15). Moreover, those authors proposed that genome acquisition occurs before the acquisition of fibrils. Our images clearly show that these events occur simultaneously (Fig. 4C and 5). It is possible that some particles receive the genome while the capsid is assembled and then the fibrils are attached, as previously proposed, but we believe that, in most cases, these events occur concomitantly.

The data presented in this study, along with previous published data based on atomic force microscopy, X-ray diffraction, and fluorescence led us to present an updated model of the replication cycle of mimiviruses (Fig. 7). Viruses enter amoeba cells by phagocytosis (0 h). After fusion of the phagosome with the lysosome (1 to 2 h), the stargate is opened and the viral seed is released (4 h). An early VF is established and viral proteins are synthesized outside the factory (4 to 6 h). In a mature VF, viral crescents increase in complexity and acquire the genome and fibrils simultaneously, as long as they move from the core of the VF to the FAA (8 h). Among the newly formed viral particles, some of them might not be infectious (defective particles), and these would exhibit morphological features similar to those in the presence of virophages (20, 22). Finally, the viral progeny is released by cell lysis. The comprehension of the biology of mimiviruses is improving due to a combination of biological and genetic data, along with increasingly illuminating images from different microscopic techniques. Notwithstanding current developments, some aspects regarding the replication

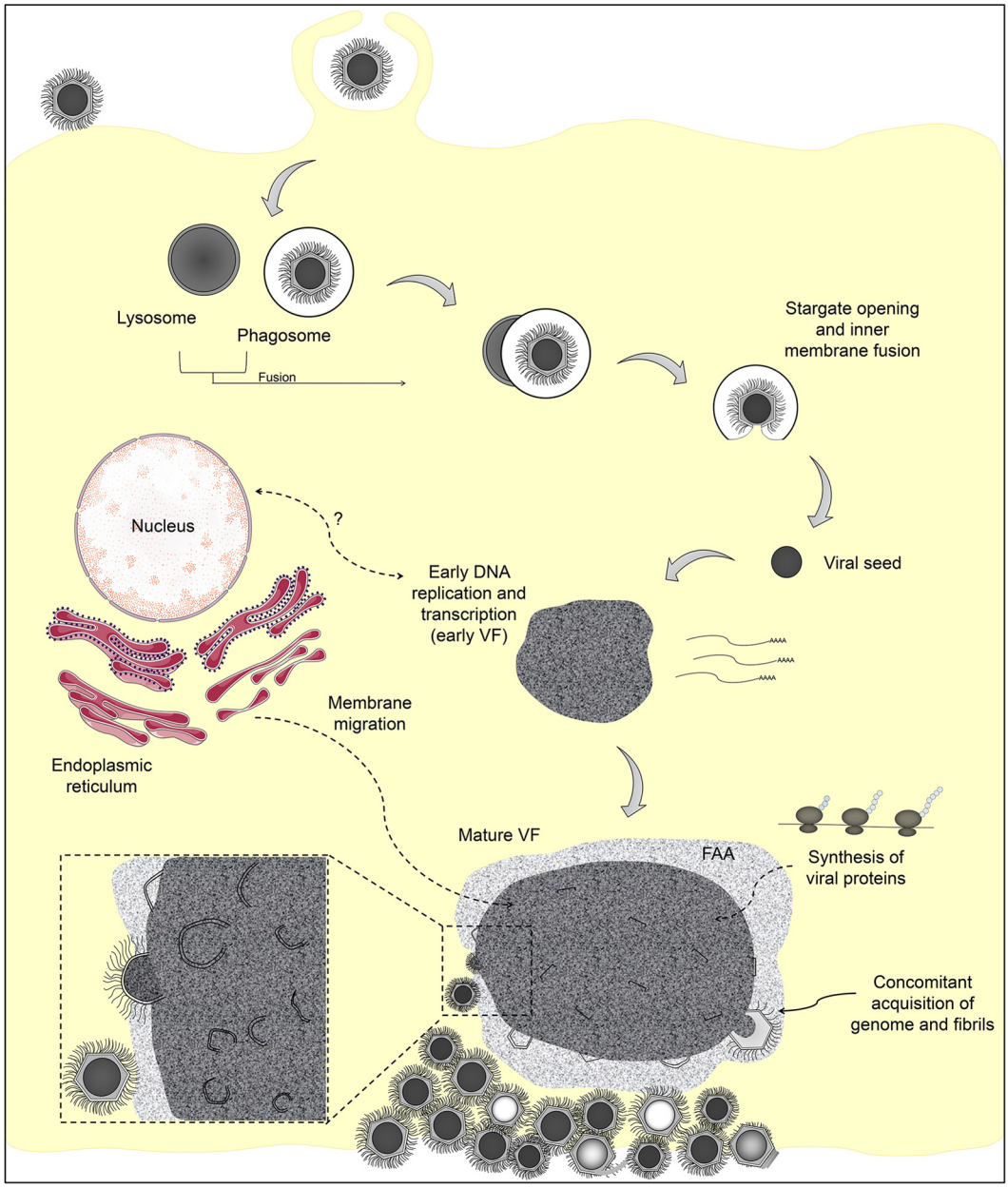

FIG 7 Representative scheme of the mimivirus replication cycle. Infectious mimivirus particles enter host cell by phagocytosis. Fusion of the phagosome with lysosome occurs and opening of the stargate is followed by release of the viral seed. An early viral factory is established, and viral proteins are synthesized outside the factory. It is uncertain whether the cell nucleus is involved in mimivirus genome replication. The viral crescents increase in thickness and complexity in the mature viral factory and might acquire genomic material and fibrils simultaneously. The particles move from the core of the viral factory to the FAA, where the particles incorporate the surface fibrils. Among the newly formed viral particles, some of them might not be infectious (defective particles), presenting atypical morphology. The viral progeny are released by cell lysis.

cycle of mimiviruses remain uncertain, and these mainly occur at the molecular level. Future studies will further enhance the model presented here and improve our understanding of the biology of these complex viruses.

MATERIALS AND METHODS

Cell culture and virus production, purification, and titration. *Acanthamoeba castellanii* (ATCC 30010) cells were cultivated in peptone-yeast extract-glucose (PYG) medium supplemented with 25 mg/ml amphotericin B (Fungizone; Cristalia, São Paulo, Brazil), 500 U/ml penicillin, and 50 mg/ml gentamicin (Schering-Plough, Brazil). A total of 7×10^6 cells were infected with APMV at an MOI of 0.01 and incubated at 32°C. After the appearance of a cytopathic effect, cells and supernatant were collected

and viruses were then purified through ultracentrifugation with a 25% sucrose cushion at 36,000 × *g* for 30 min. After purification, amoeba cells were infected with purified viruses at an MOI of 0.01. The viruses were serially diluted, and multiple replicate samples of each dilution were inoculated into *A. castellanii* (ATCC 30234) monolayers. After 72 to 96 h of incubation, the amoebas were analyzed to determine whether infection had taken place. Based on these data, the virus titers were determined using the endpoint method (30).

Transmission electron microscopy. The *Acanthamoeba castellanii* cells were infected as described in the previous section at an MOI of 0.01 and fixed at various times postinfection with 2.5% glutaraldehyde in a 0.1 M sodium phosphate buffer for 1 h at room temperature. The amoebas were postfixed with 2% osmium tetroxide and embedded in Epon resin. Ultrathin sections then were analyzed under TEM (Spirit Biotwin FEI, 120 kV).

Scanning electron microscopy. The *Acanthamoeba castellanii* cells infected at an MOI of 0.01 were added to round glass coverslips covered with poly-L-lysine and fixed with 2.5% glutaraldehyde in 0.1 M cacodylate buffer for at least 1 h at room temperature. The samples were then washed three times with 0.1 M cacodylate buffer and postfixed with 1.0% osmium tetroxide for 1 h at room temperature. After a second fixation, the samples were washed three times with 0.1 M cacodylate buffer and immersed in 0.1% tannic acid for 20 min. The samples were then washed in cacodylate buffer and dehydrated by serial passages in ethanol solutions at concentrations ranging from 35% to 100%. Samples were then subjected to critical point drying using CO_2, placed in stubs, and metallized with a 5-nm gold layer. The analyses were completed using scanning electronic microscopy (FEG Quanta 200 FEI).

Entry and uncoating assays. In the entry and uncoating experiments, we evaluated whether blocking of phagocytosis and phagosome acidification impacted APMV entry and replication. A total of 10^6 *A. castellanii* cells were treated with 2 μM cytochalasin, a phagocytosis inhibitor, in a total volume of 5 ml of PYG medium. After 1 h, supernatant was removed and cells were infected with APMV at an MOI of 5. As a negative control for the phagocytosis process, we used sonicated, purified particles of MsV under the same conditions described for APMV. It was previously demonstrated that isolated particles of MsV enter amoebas by endocytosis, not phagocytosis. Control groups of untreated, infected amoebas were also used. Two hours postinfection, the supernatant was collected to measure the remaining viral particles (nonphagocytized). The supernantant was also collected immediately after infection (0 h postinfection). The quantity of particles was calculated using flow cytometry, as previously described (31). The rate of particle incorporation was calculated, taking into consideration the variation in particle content of the supernatant between times 0 h and 2 h postinfection. An identical assay was performed in parallel, but after infection the monolayer was washed with PAS, fresh medium was added, and at 8 h postinfection amoebas were collected and titrated. The aim of this experiment was to estimate the impact on viral replication of the blocking of phagocytosis. Finally, to investigate whether blocking of cell acidification impacted APMV and MsV replication, cells were treated with 5 nM bafilomycin. Eight hours postinfection, cells were collected and titrated. All the experiments were performed three independent times, in duplicate. Graphs were constructed using GraphPad Prism version 7.00 for Windows (GraphPad Software).

ACKNOWLEDGMENTS

We thank our colleagues from Gepvig and the Laboratório de Vírus for their excellent technical support.

We also thank CNPq, CAPES, and FAPEMIG for scholarships and the Center of Microscopy of UFMG. J.S.A., C.A.B., and E.G.K. are CNPq researchers. J.S.A., E.G.K., and B.L.S. are members of a CAPES-COFECUB project.

REFERENCES

1. La Scola B, Audic S, Robert C, Jungang L, de Lamballerie X, Drancourt M, Birtles R, Claverie J-M, Raoult D. 2003. A giant virus in amoebae. Science 299:2033. https://doi.org/10.1126/science.1081867.
2. Raoult D, Audic S, Robert C, Abergel C, Renesto P, Ogata H, Scola B La, Suzan M, Claverie J-M. 2004. The 1.2-megabase genome sequence of mimivirus. Science 306:1344–1350. https://doi.org/10.1126/science.1101485.
3. Yoosuf N, Yutin N, Colson P, Shabalina SA, Pagnier I, Robert C, Azza S, Klose T, Wong J, Rossmann MG, La Scola B, Raoult D, Koonin EV. 2012. Related giant viruses in distant locations and different habitats: Acanthamoeba polyphaga moumouvirus represents a third lineage of the Mimiviridae that is close to the Megavirus lineage. Genome Biol Evol 4:1324–1330. https://doi.org/10.1093/gbe/evs109.
4. Arslan D, Legendre M, Seltzer V, Abergel C, Claverie J-M. 2011. Distant Mimivirus relative with a larger genome highlights the fundamental features of Megaviridae. Proc Natl Acad Sci U S A 108:17486–17491. https://doi.org/10.1073/pnas.1110889108.
5. Campos RK, Boratto PV, Assis FL, Aguiar ER, Silva LC, Albarnaz JD, Dornas FP, Trindade GS, Ferreira PP, Marques JT, Robert C, Raoult D, Kroon EG, La Scola B, Abrahão JS. 2014. Samba virus: a novel mimivirus from a giant rainforest, the Brazilian Amazon. Virol J 11:95. https://doi.org/10.1186/1743-422X-11-95.
6. Dornas FP, Khalil JYB, Pagnier I, Raoult D, Abrahão J, La Scola B. 2015. Isolation of new Brazilian giant viruses from environmental samples using a panel of protozoa. Front Microbiol 6:1086. https://doi.org/10.3389/fmicb.2015.01086.
7. Saadi H, Reteno DGI, Colson P, Aherfi S, Minodier P, Pagnier I, Raoult D, La Scola B. 2013. Shan virus: a new mimivirus isolated from the stool of a tunisian patient with pneumonia. Intervirology 56:424–429. https://doi.org/10.1159/000354564.
8. Xiao C, Kuznetso YG, Sun S, Hafenstein SL, Kostyuchenko VA, Chipman PR, Suzan-Monti M, Raoult D, McPherson A, Rossmann MG. 2009. Structural studies of the giant mimivirus. PLoS Biol 7:e92. https://doi.org/10.1371/journal.pbio.1000092.
9. Zauberman N, Mutsafi Y, Halevy D Ben, Shimoni E, Klein E, Xiao C, Sun S, Minsky A. 2008. Distinct DNA exit and packaging portals in the virus Acanthamoeba polyphaga mimivirus. PLoS Biol 6:1104–1114. https://doi.org/10.1371/journal.pbio.0060114.
10. Rodrigues RAL, dos Santos Silva LK, Dornas FP, de Oliveira DB, Magalhães TFF, Santos DA, Costa AO, de Macêdo Farias L, Magalhães PP,

Bonjardim CA, Kroon EG, La Scola B, Cortines JR, Abrahão JS. 2015. Mimivirus fibrils are important for viral attachment to the microbial world by a diverse glycoside interaction repertoire. J Virol 89:11812–11819. https://doi.org/10.1128/JVI.01976-15.
11. Suzan-Monti M, La Scola B, Barrassi L, Espinosa L, Raoult D. 2007. Ultrastructural characterization of the giant volcano-like virus factory of Acanthamoeba polyphaga mimivirus. PLoS One 2:e328. https://doi.org/10.1371/journal.pone.0000328.
12. Abrahão JS, Dornas FP, Silva LC, Almeida GM, Boratto PV, Colson P, La Scola B, Kroon EG. 2014. Acanthamoeba polyphaga mimivirus and other giant viruses: an open field to outstanding discoveries. Virol J 11:120. https://doi.org/10.1186/1743-422X-11-120.
13. Mutsafi Y, Zauberman N, Sabanay I, Minsky A. 2010. Vaccinia-like cytoplasmic replication of the giant mimivirus. Proc Natl Acad Sci U S A 107:5978–5982. https://doi.org/10.1073/pnas.0912737107.
14. Fridmann-Sirkis Y, Milrot E, Mutsafi Y, Ben-Dor S, Levin Y, Savidor A, Kartvelishvily E, Minsky A. 2016. Efficiency in complexity: composition and dynamic nature of mimivirus replication factories. J Virol 90:10039–10047. https://doi.org/10.1128/JVI.01319-16.
15. Kuznetsov YG, Klose T, Rossmann M, McPherson A. 2013. Morphogenesis of mimivirus and its viral factories: an atomic force microscopy study of infected cells. J Virol 87:11200–11213. https://doi.org/10.1128/JVI.01372-13.
16. Arantes TS, Rodrigues RAL, dos Santos Silva LK, Oliveira GP, de Souza HL, Khalil JYB, de Oliveira DB, Torres AA, da Silva LL, Colson P, Kroon EG, da Fonseca FG, Bonjardim CA, La Scola B, Abrahão JS. 2016. The large marseillevirus explores different entry pathways by forming giant infectious vesicles. J Virol 90:5246–5255. https://doi.org/10.1128/JVI.00177-16.
17. Yuan N, Song L, Zhang S, Lin W, Cao Y, Xu F, Fang Y, Wang Z, Zhang H, Li X, Wang Z, Cai J, Wang J, Zhang Y, Mao X, Zhao W, Hu S, Chen S, Wang J. 2015. Bafilomycin A1 targets both autophagy and apoptosis pathways in pediatric B-cell acute lymphoblastic leukemia. Haematologicaae 100:345–356. https://doi.org/10.3324/haematol.2014.113324.
18. Mutsafi Y, Shimoni E, Shimon A, Minsky A. 2013. Membrane assembly during the infection cycle of the giant mimivirus. PLoS Pathog 9:e1003367. https://doi.org/10.1371/journal.ppat.1003367.
19. Cerritelli ME, Trus BL, Smith CS, Cheng N, Conway JF, Steven AC. 2003. A second symmetry mismatch at the portal vertex of bacteriophage T7: 8-fold symmetry in the procapsid core. J Mol Biol 327:1–6. https://doi.org/10.1016/S0022-2836(03)00117-7.
20. La Scola B, Desnues C, Pagnier I, Robert C, Barrassi L, Fournous G, Merchat M, Suzan-Monti M, Forterre P, Koonin E, Raoult D. 2008. The virophage as a unique parasite of the giant mimivirus. Nature 455:100–104. https://doi.org/10.1038/nature07218.
21. Desnues C, Raoult D. 2012. Virophages question the existence of satellites. Nat Rev Microbiol 10:234. https://doi.org/10.1038/nrmicro2676-c3.
22. Gaia M, Benamar S, Boughalmi M, Pagnier I, Croce O, Colson P, Raoult D, La Scola B. 2014. Zamilon, a novel virophage with Mimiviridae host specificity. PLoS One 9:e94923. https://doi.org/10.1371/journal.pone.0094923.
23. Gong C, Zhang W, Zhou X, Wang H, Sun G, Xiao J, Pan Y, Yan S, Wang Y. 2016. Novel virophages discovered in a freshwater lake in China. Front Microbiol 7:5. https://doi.org/10.3389/fmicb.2016.00005.
24. Abrahão JS, Boratto P, Dornas FP, Silva LC, Campos RK, Almeida GM, Kroon EG, La Scola B. 2014. Growing a giant: evaluation of the virological parameters for mimivirus production. J Virol Methods 207:6–11. https://doi.org/10.1016/j.jviromet.2014.06.001.
25. Colson P, De Lamballerie X, Fournous G, Raoult D. 2012. Reclassification of giant viruses composing a fourth domain of life in the new order Megavirales. Intervirology 55:321–332. https://doi.org/10.1159/000336562.
26. Netherton CL, Wileman T. 2011. Virus factories, double membrane vesicles and viroplasm generated in animal cells. Curr Opin Virol 1:381–387. https://doi.org/10.1016/j.coviro.2011.09.008.
27. Siddiqui R, Khan N. 2012. Biology and pathogenesis of Acanthamoeba. Parasit Vectors 5:6. https://doi.org/10.1186/1756-3305-5-6.
28. Suttle CA. 2007. Marine viruses: major players in the global ecosystem. Nat Rev Microbiol 5:801–812. https://doi.org/10.1038/nrmicro1750.
29. Maruri-Avidal L, Domi A, Weisberg AS, Moss B. 2011. Participation of vaccinia virus L2 protein in the formation of crescent membranes and immature virions. J Virol 85:2504–2511. https://doi.org/10.1128/JVI.02505-10.
30. Reed LJ, Muench H. 1938. A simple method of estimating fifty per cent endpoints. Am J Hyg 27:493–497.
31. Khalil JYB, Robert S, Reteno DG, Andreani J, Raoult D, La Scola B. 2016. High-throughput isolation of giant viruses in liquid medium using automated flow cytometry and fluorescence staining. Front Microbiol 7:26. https://doi.org/10.3389/fmicb.2016.00026.